Water retained in tall Cryptomeria japonica leaves as studied by infrared micro-spectroscopy

Azuma, Wakana
Nakashima, Satoru
Yamakita, Eri
Ishii, Hiroaki
Kuroda, Keiko

Water retained in tall *Cryptomeria japonica* leaves as studied by infrared micro-spectroscopy

WAKANA AZUMA[1, 3*]

SATORU NAKASHIMA[2]

ERI YAMAKITA[2]

H. ROAKI ISHII[1]

KEIKO KURODA[1]

[1] Graduate School of Agricultural Science, Kobe University, Kobe 675-8501, Japan

[2] Graduate School of Science, Osaka University, Osaka, 560-0043, Japan

[3] Present address: Graduate School of Agriculture, Kyoto University, Kyoto 606-8502, Japan

*Author for correspondence:

Email: wakana@kais.kyoto-u.ac.jp

Phone: +81-75-753-6428

Abstract

Recent studies in the tallest tree species suggest that physiological and anatomical traits of tree-top leaves are adapted to water-limited conditions. In order to examine water retention mechanism of leaves in a tall tree, infrared (IR) micro-spectroscopy was conducted on mature leaf cross-sections of tall *Cryptomeria japonica* from four different heights (51, 43, 31 and 19 m). We measured IR transmission spectra and mainly analyzed OH (3700 – 3000 cm^{-1}) and C-O (1190 – 845 cm^{-1}) absorption bands, indicating water molecules and sugar groups respectively. The changes in IR spectra of leaf sections from different heights were compared with bulk-leaf hydraulics. Both average OH band area of the leaf sections and leaf water content were larger in the upper-crown, while osmotic potential at saturation did not vary with height suggesting higher dissolved sugar contents of upper-crown leaves. As cell-wall is the main cellular structure of leaves, we inferred that larger average C-O band area of upper-crown leaves reflected higher content of structural polysaccharides such as cellulose, hemicellulose, and pectin. IR micro-spectroscopic imaging showed that the OH and C-O band areas are large in the vascular bundle, transfusion tissue, and epidermis. IR spectra of individual tissue showed much more water is retained in vascular bundle and transfusion tissue than mesophyll. These results demonstrate that IR micro-spectroscopy is a powerful tool for visualizing detailed, quantitative information on the spatial distribution of chemical substances within plant tissues, which cannot be done using conventional methods like histochemical staining. The OH band could be well reproduced by four Gaussian OH components around 3530 (free water: long H bond), 3410 (pectin-like OH species), 3310 (cellulose-like OH species) and 3210 (bound water: short H bond) cm^{-1}, and all of these OH components were higher in the upper crown while their relative proportions did not vary with height. Based on the spectral analyses, we inferred that polysaccharides play a key role in biomolecular retention of water in leaves of tall *C. japonica*.

Keywords: water retention; hydrogen bonding; hydraulics; polysaccharides; infrared imaging; Cupressaceae

Introduction

Water transport from root to leaf via xylem in tall trees is realized by the gradient of water potential and supports vital metabolisms like photosynthesis and transpiration (Larcher 2003). As trees become tall, a gradient of light and water availabilities is formed within the crown (Koch et al. 2004, Ishii et al. 2008). At the top of tall trees, light availability for photosynthesis is high, but the water availability is physically constrained by long-distance water transport and increasing gravitational potential and hydrodynamic resistance (Ryan and Yoder 1997, Midgley 2003, Franks 2006).

In a recent study, it was found that tree-top leaves of the tallest tree species, *Sequoia sempervirens* D. Don (Cupressaceae), have capacity for foliar water storage, which may compensate for constraints on water transport from roots (Ishii et al. 2014). The same mechanism was also found in the tallest tree species in Japan, *Cryptomeria japonica* D. Don (Cupressaceae) (Azuma et al. 2016). In both species, greater water storage capacity of tree-top leaves was associated with larger volume of transfusion tissue, which is gymnosperm-specific conducting tissue surrounding the vascular bundle and has functions in water storage and transportation (Takeda 1931, Hu and Yao 1981, Brodribb et al. 2010, Oldham et al. 2010, Aloni et al. 2013, Azuma et al. 2016). These results suggest that anatomical structure of tree-top leaves is adapted to the water-limited conditions. It remains unclear, however, where and how much leaf tissues actually retain water.

Here, we used infrared (IR) micro-spectroscopy to investigate anatomical structures in leaves of tall *C. japonica* that contribute to water-retention. IR micro-spectroscopy can visualize detailed, quantitative information on where and how much various compounds reside within tissues (Gierlinger and Schwanninger 2007, Fackler et al. 2010), which cannot be done using conventional methods such as histochemical staining. IR spectroscopy has been used in plant studies such as plant anatomy, physiology and ecology (Bamba et al. 2002, Dokken et al. 2005, Ribeiro da Luz 2006, Heraud et al. 2007, Martín-Gómez et al. 2015). IR spectroscopy can visualize spatially localized distributions and relative amounts of chemical components within tissues and cells (Dokken and Davis 2007, Heraud et al. 2007). Water molecules are considered to be present in various physicochemical states because of varying hydrogen bond distances among them (Maréchal 2007). In IR spectroscopy, OH stretching absorption frequency is known to decrease with decreasing intermolecular hydrogen bond distance (Nakamoto et al. 1955). Therefore, IR OH bands are used for studying hydrogen bonding nature of water molecules associated with bio-macromolecules. Such physicochemical differences of water molecules are considered to affect physiological functions in living systems

(Nakashima et al. 2004, Maréchal 2007). Although hydrogen bonding nature of water molecules may be associated with water retention, it has not been documented in tree leaves. To investigate water retention mechanisms in the leaves of tall *C. japonica*, we measured OH and C-O absorption bands on leaf cross-sections using IR micro-spectroscopy to visualize where and how much water and sugars reside within leaf tissue. Our final goal is to elucidate molecular mechanisms of water retention within leaves. Here, we show initial results of IR micro-spectroscopy in association with physiological measurements of leaf water-relations characteristics to demonstrate application of this new technique to tree ecophysiology research.

Material and Methods

Sample collection

A 250-year-old *C. japonica* tree (height = 51 m, diameter at breast height = 114 cm) at Nibuna-Mizusawa Forest Reserve, Tashirozawa National Forest in Akita Prefecture, Japan (40.08°N, 140.25°E, 200 m altitude from sea level) was selected here as a representative tall, mature tree. In November 2013, we accessed the crown of the study tree using single-rope climbing technique. We collected small branches (30−50 cm long) from the outer crown from just below tree-top to the lowest living branches at four different heights (51, 43, 31 and 19 m). Some parts of sample branches were sealed in black plastic bags and stored in a refrigerator for IR micro-spectroscopy and the rest were used soon after sampling for physiological measurements. To quantify the light environment as canopy openness, hemispherical photographs were taken directly above each sampling location and analyzed using Gap Light Analyzer (ver 3.1, Simon Frazer University, Bernaby, BC, Canada). Canopy openness was 19.2 %, 21.8 %, 22.9%, and 83.5% at 19 m, 31 m, 43 m, and 51 m, respectively.

IR micro-spectroscopy for leaves

Second-year leaves (mature leaves) were transversely sectioned at the midpoint between leaf tip and its stem attachment to 24 μm thickness using a sliding microtome equipped with frozen mounting device (REM-710, Yamato Kohki Industrial Co., Ltd, Saitama, Japan) (Fig. 1a). Three leaves at each height were sectioned and mounted on an IR-transparent CaF_2 crystal (Fig. 1b).

In order to confirm that water in the sectioned leaves was in equilibrium with the room temperature/humidity conditions, transmission IR spectra of a leaf section sampled at 43 m height was measured at intervals of 60 seconds

using a Fourier-transform infrared (FT-IR) micro-spectrometer (FTIR-620 + IRT30, Jasco, Tokyo, Japan). A 625 μm× 625 μm aperture area in the central part of the leaf cross section (Fig.1 c,d) was monitored with 64 scans at 4 cm^{-1} resolution in the 4000 – 800 cm^{-1} region. Then at 9, 17 and 23 days after sectioning, transmission IR spectra of all leaf sections at four heights were measured using the same FT-IR micro-spectrometer with the same aperture in the central part of leaf cross sections with the same measurement conditions as above. During the measurements, room temperature and humidity were kept constant around 22 ºC and 35 %, respectively, by air conditioner. IR band area of OH (3700 – 3000 cm^{-1}) and C-O (1190 – 845 cm^{-1}) were measured with baselines set for each band region by Spectra Manager software (Jasco, Tokyo, Japan). We calculated their mean values of three leaf samples for each measurement day.

In the interval measurement of transmission IR spectra, OH band area in the sectioned leaves decreased during the first seven hours after sectioning and then became constant. IR spectra of the leaves from four different heights did not show significant changes 9, 17 and 23 days after sectioning, indicating that loss of water from the leaf sections was limited to the first several hours and water contents equilibrated with ambient humidity/temperature thereafter.

To measure microscopic distribution of water and polysaccharides over a wider area at higher spatial resolution, IR micro-spectroscopic imaging was also performed on the same leaf sections after 1 day from sectioning using an IR imaging micro-spectrometer (Nicolet iN10MX, Thermo Fisher Scientific, Yokohama, Japan) equipped with a 16 channel linear array MCT detector (1 pixel: 25 μm×25 μm). IR spectra were obtained with 1 scan in the 4000 – 800 cm^{-1} region at 16 cm^{-1} resolution. IR mapping images of the spatial distribution of band areas and peak height within the leaf cross-sections were generated using OMNIC Spectra Software (Thermo Fisher Scientific, Yokohama, Japan). To quantify IR band areas of leaf tissue, three IR spectra from mesophyll, two IR spectra from transfusion tissue, and one IR spectra from vascular bundle were selected from the IR mapping images using OMNIC Spectra Software (Thermo Fisher Scientific, Yokohama, Japan). Then, IR band area of OH (3700 – 3000 cm^{-1}) and C-O (1190 – 845 cm^{-1}) of each tissue were measured using Spectra Manager software (Jasco, Tokyo, Japan).

Identifying OH and C-O band species correlated with water retention

The IR spectrum of the leaf section at 19 m height was subtracted from those at 51, 43 and 31 m heights to discriminate different water and polysaccharide species at different heights. To normalize spectra among different heights, the 19-m spectrum was multiplied by a coefficient (1.98, 1.20, and 1.33 for 51, 43, and 31 m, respectively),

which was derived so that the difference spectra at 3000 cm^{-1} (which is considered as the stable absorption minimum) between 19 m and each height is zero. In the OH stretching region, positive bands at *c.* 3520 cm^{-1} and *c.* 3250 cm^{-1} were observed (Fig. 2b). These bands were higher for upper-crown leaves.

In IR spectroscopy, there is a large body of literature indicating strong correlations between CO, OH band areas and carbohydrate, water contents, respectively (e.g. Liang and Marchessault 1959, Olsson and Salmén 2004, Mayers et al. 2013, Kudo et al. 2017). Cellulose and pectin are two major polysaccharides in leaf tissues. To examine OH bands of cellulose and pectin, 0.5 wt. % cellulose and pectin pellets were prepared from cellulose powder (CAS No. 9004-34-6, Wako Pure Chemical Industries. Ltd.) and pectin powder (CAS No 9000-69-5, Wako Pure Chemical Industries. Ltd.) by the KBr pellets method (Smith 2011, Tonoue et al. 2014), for measuring IR transmission spectra with the same conditions as the measurement of transverse sectioned leaf using Jasco's FT-IR micro-spectrometer. The 3310 cm^{-1} band is considered to be from OH groups in cellulose, while the 3410 cm^{-1} band is from –COOH groups in pectin (Fig. 2c). As the OH band positions observed in the difference spectra of leaves (3520, 3250 cm^{-1}) and in the cellulose and pectin films (3310, 3410 cm^{-1}) were considered to be a representative OH band components of leaves, they were used as fixed positions for fitting the OH bands of leaves by four Gaussian bands to compare compositions of OH species among different heights/tissues. IR spectra of sectioned leaves were compared with those of cellulose and pectin for C-O absorption bands in the 1800 – 1000 cm^{-1}.

Relationship between OH band area and amount of water

To test the relationship between increasing OH band area and amount of water, IR spectrum and weight changes of water adsorption/desorption of a pectin film was measured simultaneously using the same FT-IR micro-spectroscopy as leaf samples and Quartz crystal microbalance (QCM-30L, SEIKO EG&G, Tokyo, Japan) under controlled relative humidity (RH, %) following methods described in Kudo et al. (2017). Pectin film was made from 0.3 wt. % pectin solution. We measured the IR spectra and weights of pectin film at RH = around 20, 30, 40, 50, 60 %, and then calculated the change in OH band area (3700 – 3000 cm^{-1}) and amount of water (μg) with the change in RH.

With increasing water adsorbed on pectin film under controlled relative humidity, the OH band area increased linearly (Fig 2, $R^2 = 0.99$, $P < 0.001$). These correlations support that (1) OH band area in IR spectra of leaves can be a good indicator of water retained in leaf tissues such as pectin and (2) water represented by the OH band area is associated with polysaccharides represented by CO band area.

Physiological measurement of leaf hydraulics

To compare the results of IR micro-spectroscopy with physiological measurements, five or six shoots comprising second- and current-year internodes were removed from sampled branches at each height for measurement of bulk leaf hydraulic properties as described in Azuma et al. (2016). Briefly, osmotic potentials at saturation (Ψ_{sat}, MPa), osmotic potential at turgor loss (Ψ_{tlp}, MPa), relative water content at turgor loss (RWC_{tlp}), and leaf capacitance (C_{leaf}, mol m^{-2} MPa^{-1}) were obtained from the pressure-volume curve using the bench drying approach (Tyree and Hammel 1972, Schulte and Hinckley 1985, Azuma et al. 2016) with a pressure chamber (Model 1000, PMS Instruments, Corvallis, OR,USA). Then, all the sample shoots were photographed for measurement of leaf surface area. The saturated leaf water content (WW, g) was calculated by subtracting the dry weight, after drying to constant weight at 65 ºC, from the fresh leaf weight at water saturation. Leaf dry weights were normalized by the leaf surface area to obtain saturated leaf water content per unit area or succulence (S_{leaf}, g H_2O m^{-2}; Bacelar et al. 2004, Ishii et al. 2014, Azuma et al. 2016).

Data analyses

We compared the effects of light environment (O_c, log transformed canopy openness) to normalize the variance) and height on IR spectra and bulk-leaf hydraulics using regression analysis, following the methods described in Coble and Cavaleri (2015). To compare IR measurements and physiological measurements, OH and C-O of IR band area were analyzed in relation to bulk-leaf hydraulics using regression analysis. OH and C-O band areas were compared among leaf tissue (mesophyll, transfusion tissue, and vascular bundle) using Tukey's HSD test (p <0.05) after regression analysis against height for each tissue. Compositions of OH species among 3530, 3410, 3210 and 3310 cm^{-1} were compared among leaf tissue using Tukey's HSD test (p <0.05) after regression analysis against height for each OH species.

Results

Fig. 3a shows IR absorbance spectra of the leaf at 51, 43, 31 and 19 m height 23 days after sectioning. Although IR spectra were measured in the 4000 – 800 cm^{-1} range, data below 900 cm^{-1} are not shown in Fig.3 due to low signals by CaF_2 window cutoff. The broad band *c.* 3325 cm^{-1} is due to OH stretching vibrations. The band with

peaks at 2920 and 2855 cm^{-1} are asymmetric and symmetric stretching of aliphatic CH_2. The band at *c.* 1740 cm^{-1} is C=O stretching of carboxyl (COOH). The band at 1640 cm^{-1} is bending mode of water molecules. The shoulder *c.* 1645 cm^{-1} could have originated from amide I (C=O stretching) of proteins. The band *c.* 1610 cm^{-1} could be due to COO^- species (deprotonated COOH). The small band *c.* 1545 cm^{-1} might be amide II (C-N-H bending, C-N stretching of peptides). The band at 1415 cm^{-1} could have originated from COO^- of pectin and that at 1370 cm^{-1} band is due to bending of aliphatic CHs. The 1320 cm^{-1} and 1235 cm^{-1} band corresponds to amide III (C-N-H bending, C-N stretching of peptides). The small band at 1315 cm^{-1} could be from OH bending in plane of alcohol group. The strong band at *c.* 1020 cm^{-1} is due to C-O species in polysaccharides. The assignments of these bands are summarized in Table 1.

When the IR spectra of sectioned leaves (Fig. 3a) was compared to that of the pectin and cellulose (Fig. 3b), the bands in the 1800 – 1000 cm^{-1}, in particular *c.* 1735 cm^{-1} (COOH) and 1610 cm^{-1} (COO^-), were similar to those for pectin but the correspondence was not clear for cellulose. In the 1800 – 1000 cm^{-1} region of the difference spectra from the leaf at 19 m height (Fig.3c), several positive bands are observed. The positive bands that are higher for upper-crown leaves include contributions mainly from 1) amide I (1670 cm^{-1}) and II (1550 cm^{-1}) bands of proteins present in mesophyll (possibly photosynthetic protein such as Rubisco), 2) COO^- of pectin (1415 cm^{-1}), and 3) C-O-C (1170 and 1120 cm^{-1}) of polysaccharides.

IR spectra and IR maps of leaf sections from different heights

OH (3700 – 3000 cm^{-1}) and C-O (1800 – 845 cm^{-1}) band areas were positively correlated with both light (O_c) and height. OH band area was more affected by light than height, while CO band area was more affected by height (Table 2). OH and C-O band areas were positively correlated with each other (Fig. 4, $R^2 = 0.54$, $P < 0.001$).

IR micro-spectroscopic imaging allowed visualization of the spatial distribution of absorption bands within leaf sections (Fig. 5). In the leaf at 19 m height, OH band area (3700 – 3000 cm^{-1}) was large in the center of the leaf, corresponding to the vascular bundle and transfusion tissue, and in epidermis (red portions in Fig. 5a). Although the leaves at 31 and 43 m showed similar distribution patterns as leaves at 19m, the image of leaves at 51 m indicated large band areas in the mesophyll regions. C-O band area (1190 – 845 cm^{-1}) in the leaf at 19 m was large around vascular bundle, transfusion tissue, and epidermis (red portions in Fig. 5b). At 31 and 43 m, the region of large C-O band area included mesophyll around the leaf periphery, and at 51 m, was widespread in all areas of the leaf. The

observed height-related patterns in OH and C-O band areas within leaf tissue explain well, the results shown in Table 2 and Fig. 4. For C-O-C bands, the ratio of 1120 cm^{-1} for 1170 cm^{-1} of polysaccharides was higher in upper-crown leaves around the vascular bundle and transfusion tissue (Fig. 5c). We discuss what it means in the Discussion part in relation to C-O band species.

A fitting result of four representative OH band components of leaves is shown in Fig. 6a. Average band areas of the four Gaussian components for three samples at each height was highest in the tree-top leaves (Fig. 6b). On the other hand, band area ratios did not vary with height (Fig. 6c). The band area of *c.* 3410 cm^{-1} (–COOH groups in pectin-like species) and *c.* 3210 cm^{-1} (water molecules with shorter H bonds) components occupy about 30%, respectively, and those of *c.* 3530 cm^{-1} (water molecules with longer H bonds) and *c.* 3310 cm^{-1} (OH groups in cellulose-like species) occupy about 20%, respectively, suggesting bound water might be more abundant than free water.

Selected IR spectra in mesophyll, transfusion tissue, and vascular

Figure 7 shows the average OH and C-O band areas of mesophyll, transfusion tissue, and vascular bundle from different heights (n = 3, 2, and 1, respectively at each height). For each tissue, both band areas show no systematic trends with height. Both band areas were largest in vascular bundle, followed by transfusion tissue and smallest in mesophyll.

Figure 8 shows the percentages of average band area ratios of mesophyll, transfusion tissue and vascular bundle (n = 3, 2 and 1 at each height, respectively) as the fitting results of representative OH band components. For each OH band components, the average band area ratios show no systematic trends with height. The band area of *c.* 3410 cm^{-1} (–COOH groups in pectin-like species) was the most abundant component in each tissue, especially in mesophyll.

Bulk-leaf hydraulics

With the exception of Ψ_{sat} and Ψ_{tlp}, bulk-leaf hydraulic properties were correlated with both light (O_c) and height (Table 2). RWC_{tlp}, WW, and S_{leaf} were more affected by light, while C_{leaf} was more affected by height. Bulk-leaf hydraulic properties, except for Ψ_{sat}, Ψ_{tlp}, and S_{leaf}, were correlated with average OH and C-O band areas (Table 3). WW was correlated with both OH and C-O band areas, while C_{leaf} and RWC_{tlp} were correlated with C-O band area.

Discussion

Our study demonstrated that IR micro-spectroscopy is a powerful tool for visualizing detailed spatial distribution of chemical substances within plant tissue. IR spectroscopy has been used for investigating hydrogen bonding in complex organic polymers such as lignin, cellulose, and hemi cellulose (e.g. Maréchal and Chanzy 2000, Olsson and Salmén 2004, Kubo and Kadla 2005, Fackler et al. 2010). While we could not elucidate how water is bound to mixed polymers within leaves, the observed height-related pattern of spatial correlation between OH and C-O band areas within leaf tissue (Figs. 4 and 5), suggest polysaccharides may contribute to water retention in tree-top leaves. Osmotic regulation in leaves is considered to be controlled mainly by dissolved sugars in plant cells (Ackerson 1981, Watanabe et al. 2000). In this study, osmotic potential of saturated leaves did not change with height, suggested larger amounts of dissolved sugars in the tree-top leaves, which have higher leaf water contents. Constant osmotic potential of saturated leaves within crown was observed during bud break in May (Azuma et al. 2016) and late season in November in this study, suggested it could be regular bulk-leaf hydraulics through the year in tall *C. japonica*. The IR spectra of 1800 – 1000 cm^{-1} region suggested that sectioned leaves contained polysaccharides, in particular pectin-like materials. Plant cell-walls consist of structural polysaccharides such as cellulose, hemicellulose and pectin whose proportions change for different species (Evert 2006, Fukushima et al. 2011). These polysaccharides are the main substances of the cellular framework. We postulate that, in the case of very thinly sliced leaves equilibrated with the ambient environmental humidity, water molecules are retained in microstructures of the cellular framework containing polysaccharides.

The results of correlations among OH band area and bulk-leaf hydraulics suggested that OH band area of IR spectrum reflected amount of water in cross-sectioned leaves, but there were no clear relationships with some measures such as Ψ_{tlp} and C_{leaf}. In tall trees, leaf hydraulics change in response to the vertical gradients of water potential, which is determined by both height via hydrostatic gradient and light via evaporative demand (Ryan and Yoder 1997, Koch et al. 2004). We found, in tall *C. japonica*, measures of water retention and storage (OH band area, RWC_{tlp}, WW, and S_{leaf}) were more affected by light than height. This may reflect physiological adaptation for maintaining leaf water status near the tree top, where the light environment is favorable for photosynthesis. Correlations of C-O band area with RWC_{tlp}, C_{leaf}, and WW suggest that some sugar species may be involved in

determining leaf hydraulic properties. Both C-O band area and C_{leaf} were more affected by height than light, suggesting physiological adaptation to the hydrostatic gradient of water potential may be achieved by increasing non-structural carbohydrate concentration in leaves.

Bamba et al. (2002) investigated the localization of polyisoprene in young stem tissues of *Eucommia ulmoides* Oliver using histochemical staining and IR micro-spectroscopy. They showed by IR micro-spectroscopy the localization and accumulation of polyisoprene in plant tissue. In our study, while conventional dye staining method (e.g., PAS staining) to visualize polysaccharides on the present leaves showed global pink coloration of the entire leaf (data not shown), IR mapping of C-O band area showed localization of polysaccharides as well as quantitative information of their relative concentrations. In addition to visualization within cross-sectioned leaf in IR maps, selected IR spectra of individual tissue showed characteristic chemical compositions of individual tissue. Among the three main water-related leaf tissues (mesophyll, transfusion tissue and vascular bundle), our results indicated much more water is retained in vascular bundle than mesophyll. The water storing function of transfusion tissue acts as a hydraulic buffer in leaves of tall *C. japonica* preventing excessive decrease in xylem water potential (Azuma et al. 2016). Here, we showed more water is retained in transfusion tissue than mesophyll. Such a gradient in water retention capacity from sink to source may function to maintain hydraulic safety of water transport within leaves.

Since pectin-like OH species is the major component particularly in mesophyll, pectin may contribute to water retention in thin cell walls and large cytoplasm of mesophyll, in contrast to thick cell walls and small conduits of vascular xylem and transfusion tissue. In a recent novel study, Bouche et al. (2016) conducted visual quantification of hydraulic failure in leaf and stem tissues to test the vulnerability segmentation hypothesis using high-resolution computed tomography, and suggested the importance of imaging techniques for vulnerability curves. Quantitative visualization of plant functional traits conducted in conjunction with measurements of dynamic, physiological responses and micro-scale anatomical structure are thus expected to provide effective new ways to study plant physiology.

Biomolecules relating to water retention

Based on inferences made by examining which OH band components are present in the OH stretching region, we present a hypothesis for biomolecular retention of water in leaves. The amount of water retained in leaves was greater for tree-top leaves, but the water species seems to be similar among different heights, indicating that

physicochemical traits of water does not change with height. This suggests higher content of water-retaining substances such as pectin- and cellulose-like compounds in tree-top leaves Considering the main C-O species detected from the difference spectra, higher content of proteins in upper-crown leaves is likely to reflect high-light acclimation for increasing photosynthetic proteins such as Rubisco (Warren and Adams 2001). The increase of COO^- possibly linked to pectin in the tree-top leaves can be explained by decarboxylation of –COOH and its binding to Ca^{2+} in the cell forming Ca^{2+} – ^-OOC linkage for cell walls of leaf tissue (Demarty et al. 1984, Liners et al. 1989, Dunand et al. 2002). The presence of positive bands from 1740 to 1610 cm^{-1} (Fig.2c) can also be explained by this conversion of COOH (1740 cm^{-1}) to COO^- (1610 cm^{-1}). The IR maps showed, for C-O-C bands, the ratio of two bands (1120 cm^{-1} for 1170 cm^{-1}) of polysaccharides was higher in upper-crown leaves around the vascular bundle and transfusion tissue (Fig. 5c). On the other hand, amounts of water and polysaccharides were greater in peripheral regions of mesophyll (Fig. 5a, b). The band around 1145 cm^{-1} for pectin (Fig.2b) can be shifted to the lower wavenumber region by hydrogen bonding of adsorbed water molecules to C-O species. Therefore, the increase in the ratio of 1120 cm^{-1} for 1170 cm^{-1} with height for mesophyll regions in the IR map (Fig. 5c) can be tentatively explained by a shift of C-O bonds by hydrogen bonding to water molecules. Thus, some changes in polysaccharides might be related to the effective radial transport and retention of water in tree-top leaves although its origin remains unknown.

As described above, Ca^{2+} ions are known to bond to deprotonated carboxyl groups (COO–) (e.g., in pectin) to form Ca bridges linking polysaccharide molecules in plant cell wall (Fig 9a, Demarty et al. 1984, Liners et al. 1989, Dunand et al. 2002). If polysaccharides are involved in water retention in leaves, one possible mechanism could be that water molecules are bound to the Ca-linked pectin molecules by hydrogen bonding to C-O-C and C-OH (Fig. 9b). Although further detailed studies for water adsorption by polysaccharides (pectin, cellulose, hemi-cellulose), lignin, proteins such as Rubisco, and lipids in leaves are needed, our observation of higher polysaccharide content in tree-top leaves suggest that a similar mechanism could explain water retention in leaves of tall trees.

Physiological significance of water retention in tall trees

In tall trees, water transport from root to tree-top is necessary for photosynthesis, and ultimately for tree growth and survival, but becomes physically difficult with increasing height. To overcome this constraint, stored water could help alleviate water stress in tree top leaves, especially if it is easily readily accessible. In *Pseudotsuga menziesii* (Mirb.) Franco var. *menziesii*, it is suggested that stem water storage plays a significant role in the water

economy with increasing tree size and helps to maintain whole trees transpiration (Phillips et al. 2003, Cermák et al. 2007). Among canopy trees in Hawaiian dry forest, stem water storage capacity was positively correlated with water transport efficiency (Stratton et al. 2000). In *S. sempervirens* and *C. japonica*, an larger amounts of stored water in leaves compensate severe water stress at tree-top (Ishii et al. 2014, Azuma et al. 2016). In young *Picea abies* L., stored water contributes to 10% and 65% of daily transpiration on sunny and cloudy days, respectively (Zweifel et al. 2001). In young *C. japonica*, stored water contributes to 10% of total daily transpiration on sunny day, more than half of which is stored in leaves (Himeno et al. in press). These studies suggest that stored water in stem and leaves play a significant role for maintaining physiological function in trees. Our results showing greater water retention in tree-top leaves of tall *C. japonica*, which are in favorable light environment give additional support to physiological acclimation of leaves to increasing height in tall trees. A novel finding of this study is that polysaccharides may be associated with water retention in leaves.

Future issues

In this study, we focused on OH absorption bands in IR spectra of cross-sectioned leaves and analyses of the detailed OH band species characteristics. The results of four OH components at different heights and tissue suggested that some changes in polysaccharides might be related to the effective radial transport and retention of water. To explain the relationship between hydrogen bonding and sugar species, we need to seek individual sugar species from C-O absorption band and investigate what C-O band species are correlated with OH band species. It is also necessary to investigate the correlation of IR bands with conventional chemical carbohydrate analyses of bulk-leaf for individual polysaccharides. In addition to osmotic regulation by dissolved sugars, water may also be bound in microstructures of the cellular framework involving Ca bridges linking pectin chains, one possible mechanism for water retention within leaves. The role of bound water in plant physiology may be elucidated by focusing on physicochemical traits of retained and transported water in future studies.

Acknowledgements

We are grateful to Ms. R. Harui of Thermo Fisher Scientific for her supports on the IR mapping measurements. We thank the Noshiro Education Board and Tohoku Forest Management Office, Ministry of Agriculture, Forestry and Fisheries for permission to conduct the research. We thank members of the Laboratory of Forest Resources, Kobe

Univ. for field assistance and Drs. A. Makita, K. Takata, K. Hoshizaki, and M. Matsushita of Akita Pref. Univ. for facilitating the study.

Funding

This research was funded by JSPS Research Fellowship to W.A. (#13J02390).

References

Ackerson RC (1981) Osmoregulation in cotton in response to water stress : II. Leaf carbohydrate status in relation to osmotic adjustment. Plant Physiol 67:489–493.

Aloni R, Foster A, Mattsson J (2013) Transfusion tracheids in the conifer leaves of *Thuja plicata* (Cupressaceae) are derived from parenchyma and their differentiation is induced by auxin. Am J Bot 100:1949–1956.

Azuma W, Ishii HR, Kuroda K, Kuroda K (2016) Function and structure of leaves contributing to increasing water storage with height in the tallest *Cryptomeria japonica* trees of Japan. Trees 30:141–152.

Bacelar EA, Correia CM, Moutinho-Pereira JM, Goncalves BC, Lopes JI, Torres-Pereira JMG (2004) Sclerophylly and leaf anatomical traits of five field-grown olive cultivars growing under drought conditions. Tree Physiol 24:233–239.

Bamba T, Fukusaki EI, Nakazawa Y, Kobayashi A (2002) In-situ chemical analyses of trans-polyisoprene by histochemical staining and Fourier transform infrared microspectroscopy in a rubber-producing plant, Eucommia ulmoides Oliver. Planta 215:934–939.

Bouche PS, Delzon S, Choat B, Badel E, Brodribb TJ, Burlett R, Cochard H, Charra-Vaskou K, Lavigne B, Li S, Mayr S, Morris H, Torres-Ruiz JM, Zufferey V, Jansen S (2016) Are needles of *Pinus pinaster* more vulnerable to xylem embolism than branches? New insights from X-ray computed tomography. Plant, Cell Environ 39: 860-870.

Brodribb TJ, Feild TS, Sack L (2010) Viewing leaf structure and evolution from a hydraulic perspective. Funct Plant Biol 37:488–498.

Cermák J, Kucera J, Bauerle WL, Phillips N, Hinckley TM, Cermak J, Kucera J, Bauerle WL, Phillips N, Hinckley TM (2007) Tree water storage and its diurnal dynamics related to sap flow and changes in stem volume in old-growth Douglas-fir trees. Tree Physiol 27:181–198.

Demarty M, Morvan C, Thellier M (1984) Calcium and the cell wall. Plant, Cell Environ 7:441–448.

Dokken KM, Davis LC (2007) Infrared imaging of sunflower and maize root anatomy. J Agric Food Chem 55:10517–10530.

Dokken KM, Davis LC, Marinkovic NS (2005) Use of infrared microspectroscopy in plant growth and development. Appl Spectrosc Rev 40:301–326.

Dunand C, Tognolli M, Overney S, Tobel L Von, Meyer M De, Simon P, Penel C (2002) Identification and characterisation of Ca^{2+}-pectate binding peroxidases in *Arabidopsis thaliana*. J Plant Physiol 1171:0–6.

Evert RF (2006) Esau's plant anatomy: meristems, cells, and tissues of the plant body: their structure, function, and development. John Wiley & Sons, New Jersey.

Fabian H, Naumann D (2012) Millisecond-to-minute protein folding/misfolding events monitored by FTIR spectroscopy. In: Fabian H, Naumann D (eds) Protein folding and misfolding. Springer, Berlin, pp 53–89.

Fackler K, Stevanic JS, Ters T, Hinterstoisser B, Schwanninger M, Salmén L (2010) Localisation and characterisation of incipient brown-rot decay within spruce wood cell walls using FT-IR imaging microscopy. Enzyme Microb Technol 47:257–267.

Franks PJ (2006) Higher rates of leaf gas exchange are associated with higher leaf hydrodynamic pressure gradients. Plant, Cell Environ 29:584–592.

Fukushima K, Funada R, Sugiyama J, Takabe K, Umezawa T, Yamamoto H (eds) (2011) Secondary xylem formation-Introduction to biomass science-2nd edition. Kaiseisha Press, Japan.

Heraud P, Caine S, Sanson G, Gleadow R, Wood BR, McNaughton D (2007) Focal plane array infrared imaging: a new way to analyse leaf tissue. New Phytol 173:216–225.

Gierlinger N, Schwanninger M (2007) The potential of Raman microscopy and Raman imaging in plant research. Spectroscopy 21:69–89.

Heraud P, Caine S, Sanson G, Gleadow R, Wood BR, McNaughton D (2007) Focal plane array infrared imaging: a new way to analyse leaf tissue. New Phytol 173:216–225.

Hu YS, Yao BJ (1981) Transfusion tissue in gymnosperm leaves. Bot J Linn Soc 83:263–272.

Ishii HR, Azuma W, Kuroda K, Sillett SC (2014) Pushing the limits to tree height: could foliar water storage compensate for hydraulic constraints in *Sequoia sempervirens*? Funct Ecol 28:1087–1093.

Ishii H, Jennings G, Sillett S, Koch G (2008) Hydrostatic constraints on morphological exploitation of light in tall

Sequoia sempervirens trees. Oecologia 156:751–763.

Kačuráková M, Wellner N, Ebringerová a, Hromádková Z, Wilson R., Belton P. (1999) Characterisation of xylan-type polysaccharides and associated cell wall components by FT-IR and FT-Raman spectroscopies. Food Hydrocoll 13:35–41.

Kačuráková M, Wilson RH (2001) Developments in mid-infrared FT-IR spectroscopy of selected carbohydrates. Carbohydr Polym 44:291–303.

Koch GW, Sillett SC, Jennings GM, Davis SD (2004) The limits to tree height. Nature 428:851–854.

Kubo S, Kadla JF (2005) Hydrogen bonding in lignin: A fourier transform infrared model compound study. Biomacromolecules 6:2815–2821.

Kudo S, Ogawa H, Yamakita E, Watanabe S, Suzuki T, Nakashima S (2017) Adsorption of water to collagen as studied using infrared (IR) microscopy combined with relative humidity control system and quartz crystal microbalance. Appl Spectrosc. doi: 10.1177/0003702817693855

Labbé N, Rials T, Kelley S, Cheng ZM, Kim JY, Li Y (2005) FT-IR imaging and pyrolysis-molecular beam mass spectrometry: New tools to investigate wood tissues. Wood Sci Technol 39:61–77.

Larcher W (2003) Physiological plant ecology: ecophysiology and stress physiology of functional groups. Springer, Berlin.

Liang CY, Marchessault RH (1959) Infrared spectra of crystalline polysaccharides. II. Native celluloses in the region from 640 to 1700 cm^{-1}. J Polym Sci 39:269–278.

Liners F, Letesson JJ, Didembourg C, Van Cutsem P (1989) Monoclonal antibodies against pectin: recognition of a conformation induced by calcium. Plant Physiol 91:1419–1424.

Maréchal Y (2007) The hydrogen bond and the water molecule: The physics and chemistry of water, aqueous and bio media. Elsevier, Netherlands.

Maréchal Y, Chanzy H (2000) The hydrogen bond network in I(β) cellulose as observed by infrared spectrometry. J Mol Struct 523:183–196.

Martín-Gómez P, Barbeta A, Voltas J, Peñuelas J, Dennis K, Palacio S, Dawson TE, Ferrio JP (2015) Isotope-ratio infrared spectroscopy: a reliable tool for the investigation of plant-water sources? New Phytol 207:914–927.

Mayers J, Flynn KJ, Shields RJ, Mayers JJ, Flynn KJ, Shields RJ (2013) Rapid determination of bulk microalgal biochemical composition by Fourier-Transform Infrared spectroscopy. Bioresour Technol 148:215–220.

Midgley JJ (2003) Is bigger better in plants? The hydraulic costs of increasing size in trees. Trends Ecol Evol 18:5–6.

Nakamoto K, Margoshes M, Rundle RE (1955) Stretching frequencies as a function of distances in hydrogen bonds. J Am Chem Soc 77:6480–6486.

Nakashima S, Spiers C., Mercury L, Fenter P., Hochella M. (eds) (2003) Physicochemistry of water in geological and biological systems-Structures and properties of thin aqueous films. Universal Academy Press, Inc., Tokyo, Japan.

Oldham AR, Sillett SC, Tomescu AMF, Koch GW (2010) The hydrostatic gradient, not light availability, drives height-related variation in *Sequoia sempervirens* (Cupressaceae) leaf anatomy. Am J Bot 97:1087–1097.

Olsson AM, Salmén L (2004) The association of water to cellulose and hemicellulose in paper examined by FTIR spectroscopy. Carbohydr Res 339:813–818.

Painter P, Snyder R, Starsinic M, Coleman M, Kuehn D, Davis A (1981) Concerning the application of FT-IR to the study of coal: A critical assessment of band assignments and the application of spectral analysis programs. Appl Spectrosc 35:475–485.

Phillips, Ryan MG, Bond BJ, McDowell NG, Hinckley TM, Cermak J (2003) Reliance on stored water increases with tree size in three species in the Pacific Northwest. Tree Physiol 23:237–245.

Ribeiro da Luz B (2006) Attenuated total reflectance spectroscopy of plant leaves: A tool for ecological and botanical studies. New Phytol 172:305–318.

Ryan MG, Yoder BJ (1997) Hydraulic limits to tree height and tree growth: what keeps trees from growing beyond a certain height? Bioscience 47:235–242.

Schulte PJ, Hinckley TM (1985) A comparison of pressure-volume curve data analysis techniques. J Exp Bot 36:1590–1602.

Smith BC (2011) Fundamentals of Fourier transform infrared spectroscopy Smith BC (ed), 2nd edn. CRC Press, Taylor & Francis Group.

Stratton L, Goldstein G, Meinzer FC (2000) Stem water storage capacity and efficiency of water transport: their functional significance in a Hawaiian dry forest. Plant Cell Environ 23:99–106.

Synytsya A, Copikova J, Matejka P, Machovic V (2003) Fourier transform Raman and infrared spectroscopy of pectins. Carbohydr Polym 54:97–106.

Szymanska-Chargot M, Zdunek A (2013) Use of FT-IR Spectra and PCA to the Bulk Characterization of Cell Wall

Residues of Fruits and Vegetables Along a Fraction Process. Food Biophys 8:29–42.

Takeda H (1931) A theory of 'transfusion-tissue'. Ann Bot os-27:359–363.

Tonoue R, Katsura M, Hamamoto M, Bessho H, Nakashima S (2014) A method to obtain the absorption coefficient spectrum of single grain coal in the aliphatic C-H stretching region using infrared transflection microspectroscopy. Appl Spectrosc 68:733–739.

Tyree MT, Hammel HT (1972) The measurement of the turgor pressure and the water relations of plants by the pressure-bomb technique. J Exp Bot 23:267–282.

Warren CR, Adams M a. (2001) Distribution of N, Rubisco and photosynthesis in *Pinus pinaster* and acclimation to light. Plant, Cell Environ 24:597–609.

Watanabe S, Kojima K, Ide Y, Sasaki S (2000) Effects of saline and osmotic stress on proline and sugar accumulation in *Populus euphratica* in vitro. Plant Cell Tissue Organ Cult 63:199–206.

Yang H, Yan R, Chen H, Lee DH, Zheng C (2007) Characteristics of hemicellulose, cellulose and lignin pyrolysis. Fuel 86:1781–1788.

Zweifel R, Hasler R (2001) Dynamics of water storage in mature subalpine *Picea abies*: temporal and spatial patterns of change in stem radius. Tree Physiol 21:561–569.

Zweifel R, Item H, Häsler R (2001) Link between diurnal stem radius changes and tree water relations. Tree Physiol 21:869–877.

Figure legends

Fig. 1 Procedures for IR micro-spectroscopy of *Cryptomeria japonica* leaves.

(a) Sampling and transverse sectioning of leaves. b) Mounting of sections on CaF_2. (c) A microphoto of a transvers section. (d) A magnified central area of 625x625 μm^2 used for IR measurement.

Fig. 2 Correlation between increase in amount of water (weight increase: μg) by quartz crystal microbalance and increase in IR OH band area on a pectin film with increasing relative humidity (RH) from 20 to 30, 40, 50 and 60 %.

Fig. 3 (a) IR absorbance spectra of the leaves at 19, 31, 43 and 51 m, 23 days after sectioning. (b) IR absorbance spectra of cellulose and pectin powders by KBr pellet method. (c) Difference spectra from the 19 m spectrum with a coefficient so as to obtain the absorbance zero at 3000 cm^{-1} (51m spectrum: 51 m – 19 m x 1.98, 43 m: 43 m – 19 m x 1.2, 31 m: 31 m – 19 m x1.33) to discriminate water and polysaccharide species at different heights. The assignments of bands are summarized in Table 1.

Fig. 4 Correlation between band areas of C-O (1190-845 cm^{-1}) and OH (3700-3000 cm^{-1}) within cross-sectioned leaves.

Fig. 5 IR micro-spectroscopic mapping images of leaf sections from different heights for (a) OH band area (3700-3000 cm^{-1}, abs: 0-150), (b) C-O band area (1190-845 cm^{-1}, abs: 0-50) and (c) peak height ratio of 1120 cm^{-1} for 1170 cm^{-1} (C-O-C bands, baseline: 1190-845 cm^{-1}, abs: 0-9). Water and polysaccharides was larger in mesophyll region of 51m leaves. Change of peak height ratio with height can be tentatively explained by a shift of C-O bonds by hydrogen bonding to water molecules, suggested polysaccharides may contribute to water retention in upper-crown leaves around the vascular bundle and transfusion tissue.

Fig. 6 (a) A representative curve fitting result of OH band by four Gaussian components with initial band positions at 3530 (water molecules with longer H bonds), 3410 (–COOH groups in pectin-like species), 3310 (OH groups in cellulose-like species) and 3210 cm^{-1} (water molecules with shorter H bonds) of a leaf at 43m. Bound water might be more abundant than free water. (b) Band areas of four OH band species was larger in upper-crown leaves. Error bars indicate maximum and minimum value ranges. (c) Average band area ratios (percentages in the total band areas) of four OH band areas did not vary with height.

Fig. 7 OH and C-O band areas in mesophyll, transfusion tissue and vascular bundle regions extracted from the IR mapping results for different heights. Different letters denote significant differences among tissues ($p < 0.05$,

ANOVA followed by Tukey's HSD test).

Fig. 8 Average band area ratios (percentages in the total band areas) of four OH species (free, pectin-like, cellulose-like and bound water) for mesophyll, transfusion tissue and vascular bundle regions extracted from the IR mapping results for different heights. Different letters denote significant differences among OH species ($p < 0.05$, ANOVA followed by Tukey's HSD test).

Fig. 9 A working hypothesis for biomolecular mechanism of water retention in leaves of tall trees. (a) The carboxyl groups (COOH) become deprotonated (COO-) and bound to Ca^{2+} in the cell to form Ca bridges linking pectin chains. (b) Water molecules are then bound in the Ca-linked pectin molecules by hydrogen bonding to C-O-C and C-OH (Modified from Fukushima et al. (2011)).

Table 1 Assignments of infrared bands observed in transmission spectra of the leaf section at 43 m (Fig.3a), in the spectra for pectin and cellulose films (Fig.3b), in the difference spectra from the 19 m spectrum for the leaves at 51, 43 and 31 m (Fig.3c) and in the OH bands of the leaves (Fig.6).

Fig. No.	Wavenumber (cm^{-1})	Assignment	Ref #
3c, 6	3530	ν(O-H) (long H bond)	8, 13
3b, 6	3410	ν(O-H) (COOH of pectin)	6
3b, 6	3310	ν(O-H) (OH of cellulose)	7, 11
3c, 6	3210	ν(O-H) (short H bond)	13, 18
3a	2920	ν_{as}(C-H) from aliphatic CH_2	2, 17
3a	2855	ν_s(C-H) from aliphatic CH_2	2, 17
3a, b, c	1740, 1735	ν(C=O) (COOH of pectin, lignin and lipids)	2, 5, 6, 9, 12, 15, 17
3a, c	1670, 1645	ν(C=O) from peptides (H-N-C=O) (amide I of proteins)	12, 14, 18
3b	1640	δ(H-O-H) of water molecules	3, 5, 10
3a, b	1610, 1625	ν(C=O) of lignin, ν_{as}(COO-) of pectin	5, 6, 12,
3a, c	1550, 1545	ν(C-N) and δ(N-H) from amide II of proteins	12, 14, 18
3c	1515	ν(C=C) of lignin	12
3b, c	1450, 1440	$\delta_{as}(CH_3)$ and $\delta_{as}(CH_2)$ of proteins, lipids and lignin	2, 12,
3a, c	1415	$\nu_s(COO^-)$ of pectin	5, 6, 12, 15
3b, c	1375	δ(C-H) from CH_3 groups	2, 17
3a	1370	$\delta_s(CH_3)$ and $\delta_s(CH_2)$ of proteins, lipids and lignin	12
3b	1330	ν(O-H) from COH alcohol groups of cellulose	4
3a, c	1320, 1235	ν(C-N) and δ(N-H) from amide III of proteins	12, 14
3a, b	1315	δ(O-H) in plane from alcohol groups of carbohydrates	4, 13
3c	1270	ν(C-C) and ν(C-O) of carbohydrates and lignin	12
3b, c	1170, 1150	ν_{as}(C-O-C) from glycoside of polysaccharides	1, 3, 4, 9, 13
3b	1145	ν_{as}(C-O-C) of pectin	6, 12
3c	1120	ν_{as}(C-O-C) in ring of polysaccharides	1, 3, 4
3b	1100	ν_s(COOH) of polysaccharides	10
3a, b	1020, 1030, 1050	ν(C-O) of polysaccharides and cellulose	4, 10, 13

Abbreviations designate the followings. ν_{as}: asymmetric stretch, ν_s: symmetric stretch, δ_{as}: asymmetric deformation (bend), δ_s: symmetric deformation (bend).

Band assignments are taken from references Liang and Marchessault (1959)[1], Painter et al. (1981)[2], Kačuráková et al. (1999)[3], Maréchal and Chanzy (2000)[4], Kačuráková and Wilson (2001)[5], Synytsya et al. (2003)[6], Chung et al. (2004)[7], Kubo and Kadla (2005)[8], Labbé et al. (2005)[9], , Ribeiro da Luz (2006)[10], Yang et al. (2007)[11], Heraud et al. (2007)[12], Fackler et al. (2010)[13], Fabian and Naumann (2012)[14], Szymanska-Chargot and Zdunek (2013)[15], Mayers et al. (2013)[16], Tonoue et al. (2014)[17], Kudo et al. (2017)[18].

Table 2 Results of regression analyses of IR band areas and bulk-leaf hydraulics in relation to canopy openness (O_C) and height (H).

Respose variable	(a) Light only				(b) Height only				(c) Light and Height					Partial R^2 for adding:	
	β_0		β_1	R^2	β_0		β_1	R^2	β_0		β_1	β_2	R^2	Light	Height
OH band area	-47.6	*	32.1 ***	0.870	13.9		1.32 **	0.593	-43.1	**	28.2 ***	0.239	0.866	**0.273**	-0.005
C-O band area	6.09		7.72 ***	0.680	17.0	***	0.423 ***	0.894	12.4	**	2.27	0.336 ***	0.911	0.017	**0.231**
Ψ_{sat}	-1.92	**	0.189	0.026	-1.48	***	0.006	-0.052	-1.99	**	0.254	-0.004	-0.071	-0.020	-0.098
Ψ_{tlp}	-2.56	***	0.143	0.142	-2.27	***	0.005	0.049	-2.56	***	0.144	0.000	0.047	-0.002	-0.095
RWC_{tlp}	0.57	***	0.049 ***	0.666	0.658	***	0.002 ***	0.629	0.60	***	0.030	0.001	0.709	**0.080**	0.043
C_{leaf}	0.11		0.205 *	0.318	0.375	*	0.012 **	0.505	0.32		0.029	0.011	0.454	-0.051	**0.136**
WW	-0.01		0.038 *	0.395	0.062	*	0.002 *	0.322	0.01		0.027	0.001	0.354	**0.033**	-0.040
S_{leaf}	26.8		29.0 **	0.472	74.9	***	1.39 **	0.462	41.1		16.7	0.755	0.484	**0.021**	0.011

Model equations: (a) $y = \beta_0 + \beta_1 \ln(O_C)$, (b) $y = \beta_0 + \beta_1 H$, (c) $y = \beta_0 + \beta_1 \ln(O_C) + \beta_2 H$. * $p < 0.05$, ** $p < 0.01$, *** $p < 0.001$

Table 3 Correlations of OH (3700-3000 cm^{-1}) and C-O (1190-845 cm^{-1}) IR band areas with some bulk-leaf hydraulics. Bold represents $p < 0.05$.

	Ψ_{sat}		Ψ_{tlp}		RWC_{tlp}		C_{leaf}		WW		S_{leaf}	
	R	p-value	R	p-value	R	p-value	R	p-value	R	p-value	R	p-value
OH band area	0.94	0.06	0.91	0.09	0.89	0.11	0.80	0.20	0.97	**0.03**	0.75	0.25
C-O band area	0.70	0.30	0.86	0.14	0.96	**0.04**	0.98	**0.02**	0.96	**0.04**	0.89	0.11

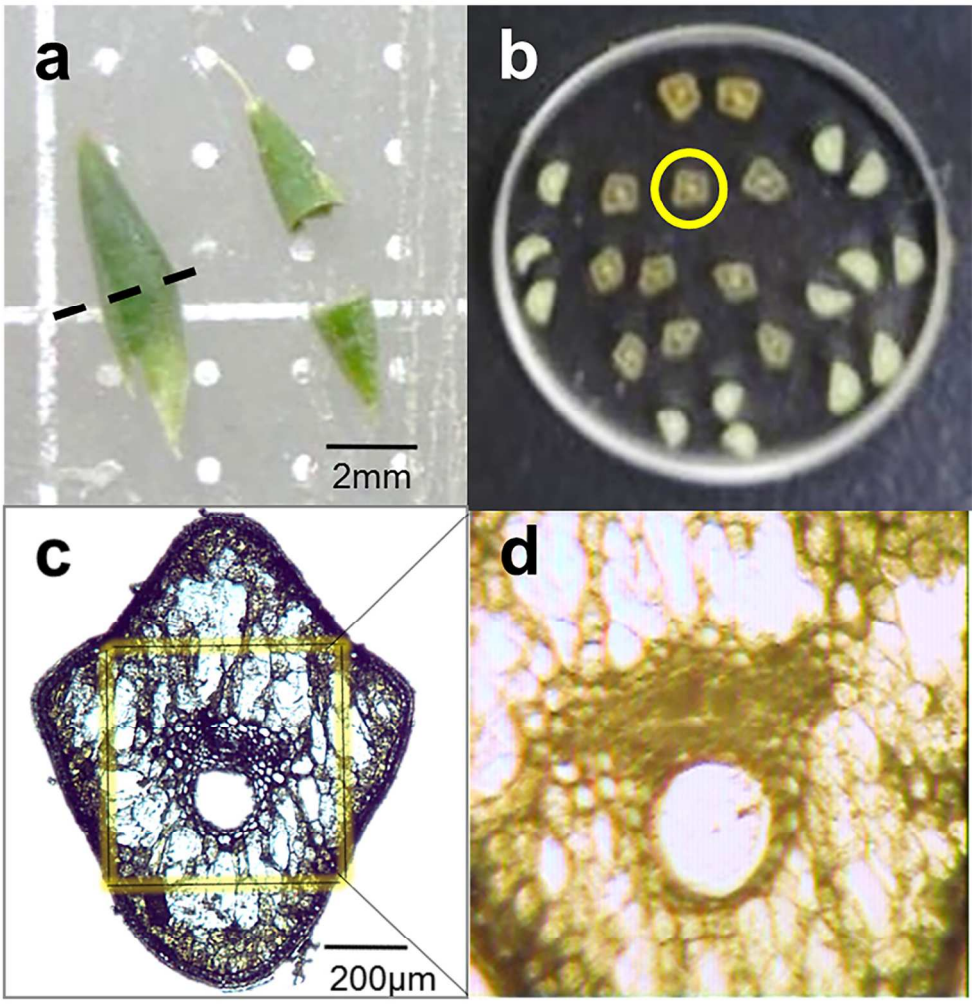

Fig. 1 Procedures for IR micro-spectroscopy of *Cryptomeria japonica* leaves.
(a) Sampling and transverse sectioning of leaves. b) Mounting of sections on CaF_2. (c) A microphoto of a transvers section. (d) A magnified central area of 625x625 μm^2 used for IR measurement.

129x135mm (300 x 300 DPI)

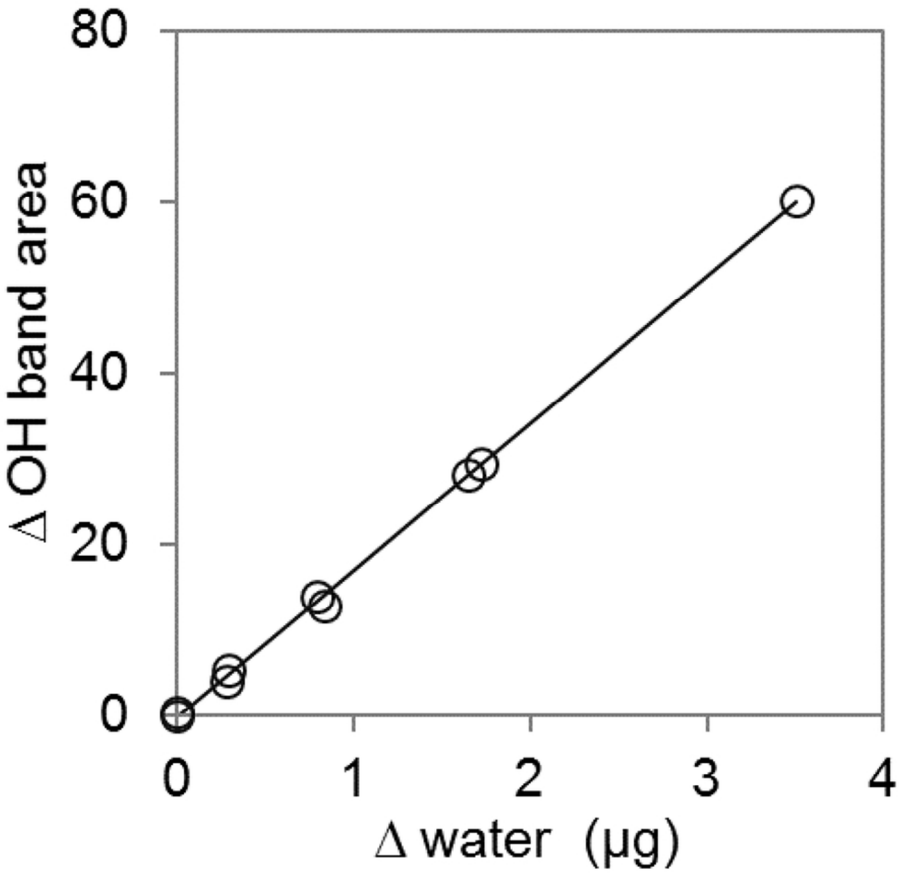

Fig. 2 Correlation between increase in amount of water (weight increase: μg) by quartz crystal microbalance and increase in IR OH band area on a pectin film with increasing relative humidity (RH) from 20 to 30, 40, 50 and 60 %.

84x77mm (300 x 300 DPI)

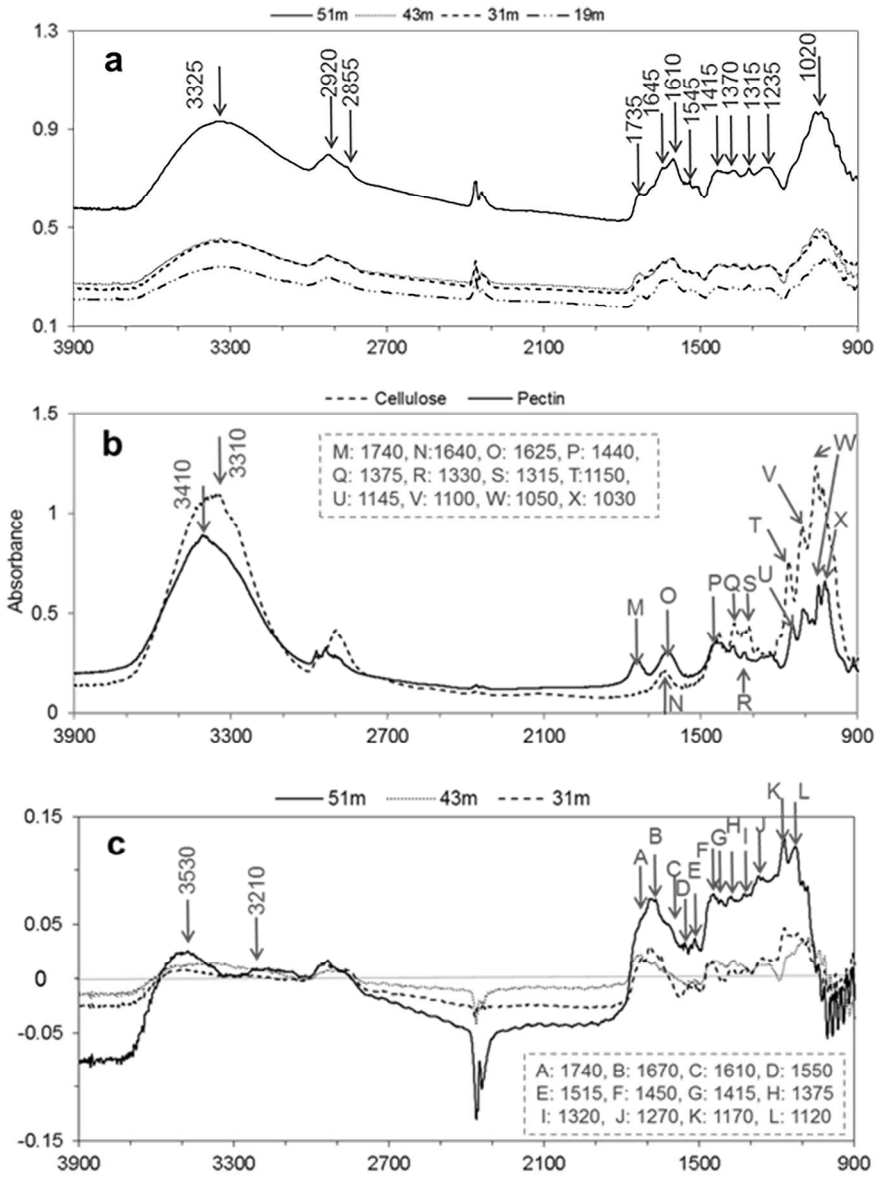

Fig. 3 (a) IR absorbance spectra of the leaves at 19, 31, 43 and 51 m, 23 days after sectioning. (b) IR absorbance spectra of cellulose and pectin powders by KBr pellet method. (c) Difference spectra from the 19 m spectrum with a coefficient so as to obtain the absorbance zero at 3000 cm-1 (51m spectrum: 51 m – 19 m x 1.98, 43 m: 43 m – 19 m x 1.2, 31 m: 31 m – 19 m x1.33) to discriminate water and polysaccharide species at different heights. The assignments of bands are summarized in Table 1.

206x270mm (300 x 300 DPI)

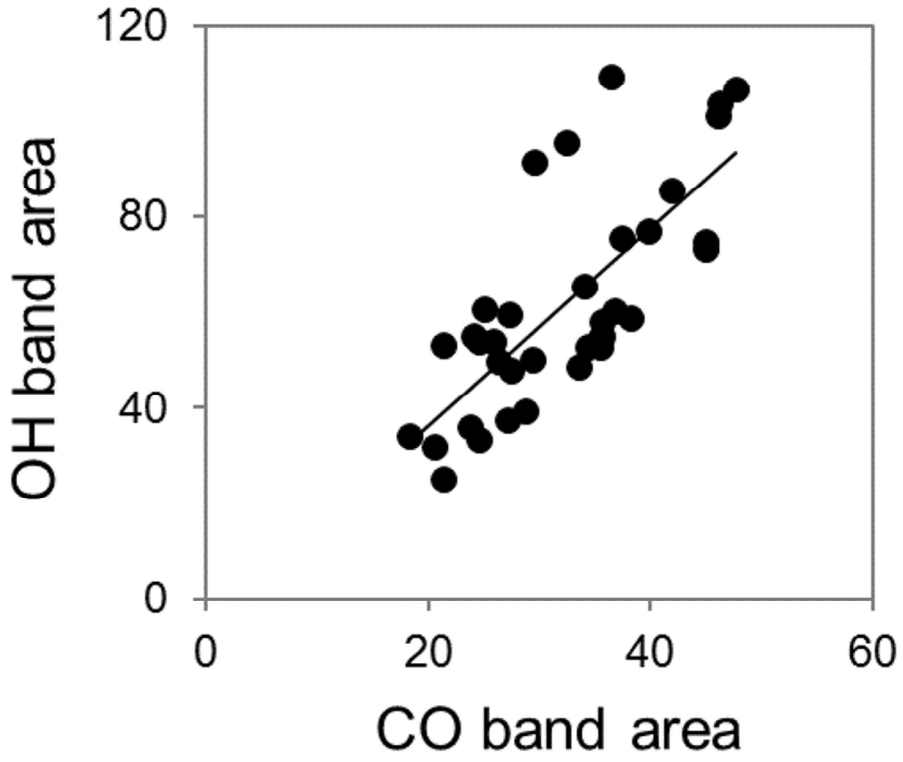

Fig. 4 Correlation between band areas of C-O (1190-845 cm^{-1}) and OH (3700-3000 cm^{-1}) within cross-sectioned leaves.

78x64mm (300 x 300 DPI)

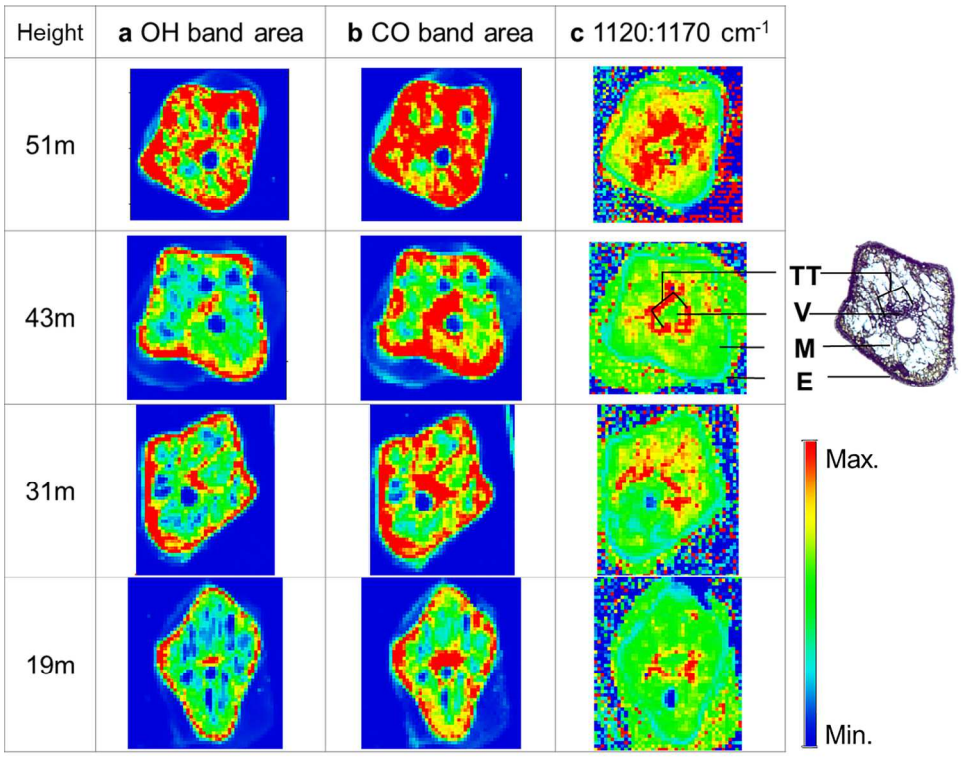

Fig. 5 IR micro-spectroscopic mapping images of leaf sections from different heights for (a) OH band area (3700-3000 cm^{-1}, abs: 0-150), (b) C-O band area (1190-845 cm^{-1}, abs: 0-50) and (c) peak height ratio of 1120 cm^{-1} for 1170 cm^{-1} (C-O-C bands, baseline: 1190-845 cm^{-1}, abs: 0-9). Water and polysaccharides was larger in mesophyll region of 51m leaves. Change of peak height ratio with height can be tentatively explained by a shift of C-O bonds by hydrogen bonding to water molecules, suggested polysaccharides may contribute to water retention in upper-crown leaves around the vascular bundle and transfusion tissue.

162x123mm (300 x 300 DPI)

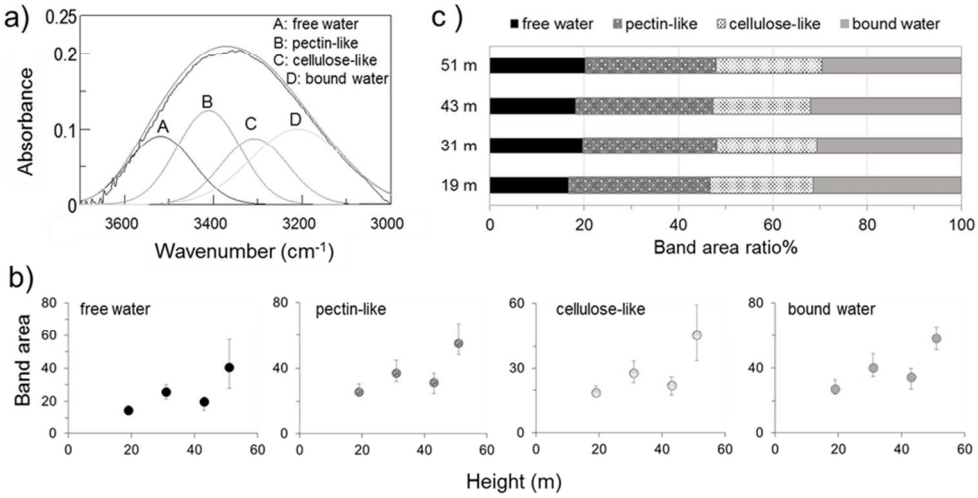

Fig. 6 (a) A representative curve fitting result of OH band by four Gaussian components with initial band positions at 3530 (water molecules with longer H bonds), 3410 (–COOH groups in pectin-like species), 3310 (OH groups in cellulose-like species) and 3210 cm^{-1} (water molecules with shorter H bonds) of a leaf at 43m. Bound water might be more abundant than free water. (b) Band areas of four OH band species was larger in upper-crown leaves. Error bars indicate maximum and minimum value ranges. (c) Average band area ratios (percentages in the total band areas) of four OH band areas did not vary with height.

83x46mm (300 x 300 DPI)

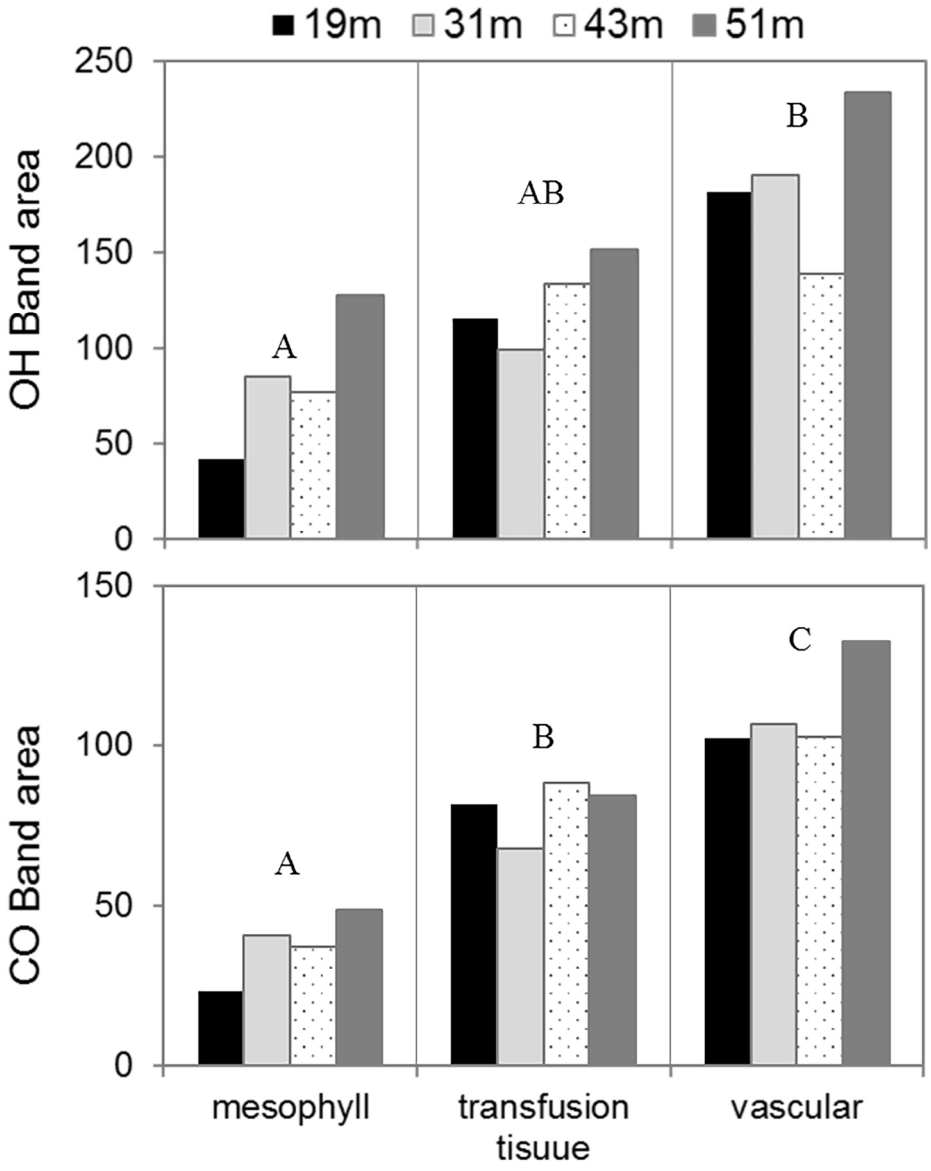

Fig. 7 OH and C-O band areas in mesophyll, transfusion tissue and vascular bundle regions extracted from the IR mapping results for different heights. Different letters denote significant differences among tissues ($p < 0.05$, ANOVA followed by Tukey's HSD test).

144x179mm (300 x 300 DPI)

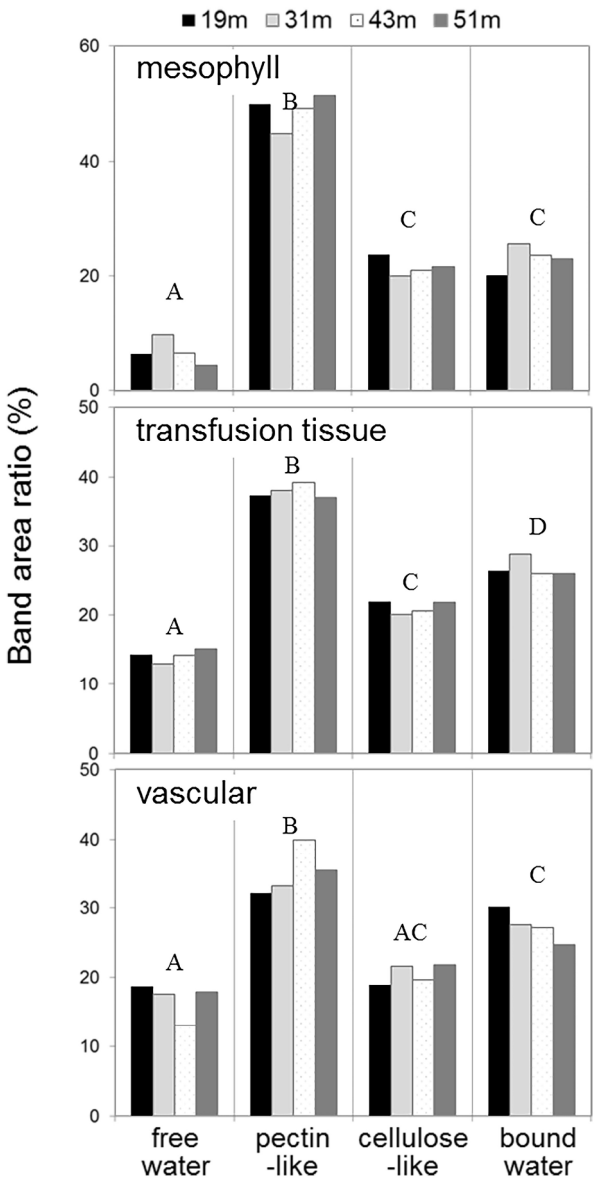

Fig. 8 Average band area ratios (percentages in the total band areas) of four OH species (free, pectin-like, cellulose-like and bound water) for mesophyll, transfusion tissue and vascular bundle regions extracted from the IR mapping results for different heights. Different letters denote significant differences among OH species ($p < 0.05$, ANOVA followed by Tukey's HSD test).

183x357mm (300 x 300 DPI)

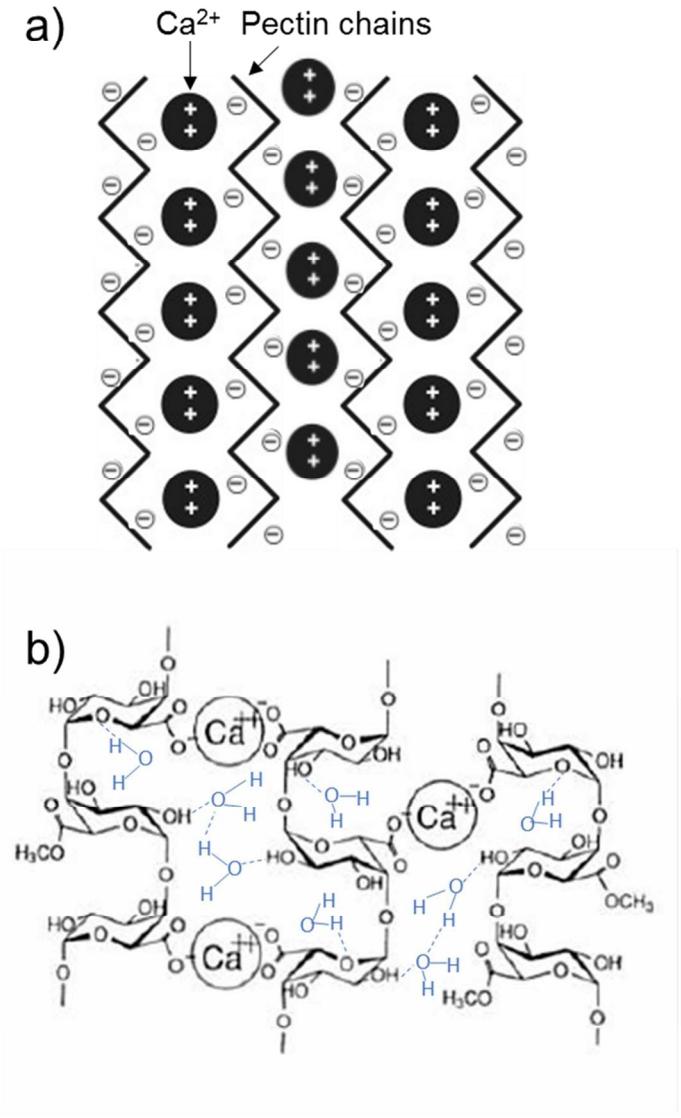

Fig. 7 A working hypothesis for biomolecular mechanism of water retention in leaves of tall trees. (a) The carboxyl groups (COOH) become deprotonated (COO-) and bound to Ca^{2+} in the cell to form Ca bridges linking pectin chains. (b) Water molecules are then bound in the Ca-linked pectin molecules by hydrogen bonding to C-O-C and C-OH (Modified from Fukushima et al. (2011)).

101x125mm (300 x 300 DPI)